



Review

# Supplementary Information: Recent PELE Developments and Applications in Drug Discovery Campaigns

Ignasi Puch-Giner <sup>1</sup>, Alexis Molina <sup>2</sup>, Martí Municoy <sup>1,2</sup>, Carles Pérez <sup>2</sup> and Victor Guallar <sup>1,2,\*</sup>

<sup>1</sup> Barcelona Supercomputing Center, Plaça d'Eusebi Güell, 1-3, 08034 Barcelona, Spain

<sup>2</sup> Nostrum Biodiscovery S.L., Av. de Josep Tarradellas, 8-10, 3-2, 08029 Barcelona, Spain

\* Correspondence: victor.guallar@bsc.es

## 1. Methods

### 1.1. System Preparation

For each system, crystals with missing atoms in side chains or missing loops were corrected with Maestro and its 3D Builder [48]. To determine the connectivity and the protonation states we used the Protein Preparation Wizard from Schrödinger [49] as well as PROPKA [50] at the pH at which the crystallization of the complex had been done.

### 1.2. AquaPELE and fragPELE Simulation Protocol

OPLS2005 [13] force field was used to parameterize protein residues for both aquaPELE simulations and Frag + aquaPELE simulations. We used the SGB solvent model [51] in the implicit/explicit solvent protocol in aquaPELE simulations. We set the aquaPELE simulations to explore the possible ligand conformations and hydrated sites within the receptor's binding site. We performed 47 parallel simulations of 400 Monte Carlo steps (18.800 total steps). The fragment growth was implemented in 10 growing epochs of 6 Monte Carlo steps each. The final sampling simulation consisted of 400 Monte Carlo steps, comparable to the scaffold-alone simulation.

### 1.3. Clustering to Characterize Hydration Sites

A heavy-atom mean-shift clustering was used to discern the most populated and important spatial regions for both the ligand and the water molecules. We characterized the hydration sites in four steps:

1. First, out of all the snapshots in each simulation, we clustered the ligand's positions to see which conformations were the most frequent.
2. Out of all the clusters we picked the most populated.
3. We kept the snapshots that belonged to said cluster.
4. From the snapshots, we tracked the positions of the perturbable waters to cluster their most frequent positions.
5. Finally we obtained a representative position of the most populated water clusters.

### 1.4. Scoring Metrics for Energetic Benchmark

- P5: Average binding energy of 5th percentile of all the simulation.
- POP5: Average binding energy of 5th percentile of all snapshots belonging to the most populated ligand cluster.
- P25: Average binding energy of 25th percentile of all the simulation.
- POP25: Average binding energy of 25th percentile of all snapshots belonging to the most populated ligand cluster.
- MBE: Average binding energy of all the simulation.
- POPMBE: Average binding energy of all snapshots belonging to the most populated ligand cluster.



**Citation:** Puch-Giner, I.; Molina, A.; Municoy, M.; Pérez, C.; Guallar, V. Recent PELE Developments and Applications in Drug Discovery Campaigns. *Int. J. Mol. Sci.* **2022**, *23*, 16090. <https://doi.org/10.3390/ijms232416090>

Received: 18 November 2022

Accepted: 13 December 2022

Published: 17 December 2022

**Publisher's Note:** MDPI stays neutral with regard to jurisdictional claims in published maps and institutional affiliations.



**Copyright:** © 2022 by the authors. Licensee MDPI, Basel, Switzerland. This article is an open access article distributed under the terms and conditions of the Creative Commons Attribution (CC BY) license (<https://creativecommons.org/licenses/by/4.0/>).

## 2. Images and Tables

**Table S1.** Structural information of all fixed water molecules for each system according to the labelling of the indicated PDB.

Systems		PDB scaffold	Fixed Waters IDs
HSP90 (1)		3RLQ	237,258,313,243,231
HSP90 (2)		2XAB	2118,2155
BRD4		5I80	352,364
TAF1		5I29	1832,1882
SiaP WT		2V4C	2198,2016,2088,2343, 2253,2037,2228,2251,2110, 2109,2226,2344,2345
CHK1		2C3L	-
Control	HSP90 (1)	3RLQ	237,258,313,243,231
	HSP90(3)	-	261,297,372,311, 336,292,229,274,310, 370,230,240,244



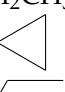
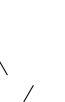



**Table S2.** Set of grown fragments from the original scaffold L1 (Supplementary Figure S2). Their respective energetic toll has been calculated with the experimental  $K_i$  with  $\Delta\Delta G = k_B T \ln(K_i)$ .

Compound	L1			$\Delta\Delta G$ (kcal mol <sup>-1</sup> )
	R1	R2	R3	
Kung-4	OCH <sub>3</sub>	H	H	-6.95
Kung-5	OCH <sub>3</sub>	Cl	H	-7.59
Kung-6	Cl	Cl	H	-8.80
Kung-7	Cl	Cl	OCH <sub>3</sub>	-9.34

**Table S3.** Set of grown fragments from the original scaffold L2 (Supplementary Figure S2). Their respective energetic toll has been calculated with the experimental  $K_i$  with  $\Delta\Delta G = k_B T \ln(K_i)$ .

Compound	L2		$\Delta\Delta G$ (kcal mol <sup>-1</sup> )
	R1	R2	
Kung-10	COCH <sub>3</sub>	H	-9.13
Kung-11	F	H	-9.13
Kung-12	Cl	H	-9.13
Kung-13	CN	H	-10.08
Kung-14	H	CH <sub>3</sub>	-7.77
Kung-15	Cl	CH <sub>3</sub>	-9.54
Kung-16	CN	CH <sub>3</sub>	-10.25
Kung-17	CN	CH <sub>2</sub> CH <sub>3</sub>	-10.66

**Table S4.** Set of grown fragments from the original scaffold L3 (Supplementary Figure S2). Their respective energetic toll has been calculated with the experimental  $K_i$  with  $\Delta\Delta G = k_B T \ln(K_i)$ .

Compound	L3				$\Delta\Delta G$ (kcal mol <sup>-1</sup> )
	R1	R2	R3	R4	
Woodhead-2		H	H	H	-12.63
Woodhead-5		H	H	CH <sub>3</sub>	-10.66
Woodhead-6	CH <sub>2</sub> CH <sub>3</sub>	H	H	H	-11.85
Woodhead-7		H	H	H	-11.44
Woodhead-8		H	H	H	-11.61
Woodhead-9		H	H	H	-12.26
Woodhead-10	Cl	H	H	H	-11.44
Woodhead-11		H	F	H	ND
Woodhead-12		F	H	H	ND

**Table S5.** Correlation between the experimental data in the literature and predicted data depending on the protocol (W, FW, NW) and the scoring method for the first series of congeneric ligands (L1). These correlations were calculated with four data points corresponding to each fragment-grown compound in Supplementary Table S2.

Serie 1 (L1)			
Scoring method	r(W)	r(FW)	r(NW)
P5	0.98	0.96	0.71
P25	0.97	0.93	0.72
MBE	0.92	0.91	0.75
POP5	0.99	0.96	0.76
POP25	0.97	0.93	0.78
POPMBE	0.92	0.91	0.76

**Table S6.** Correlation between the experimental data in the literature and predicted data depending on the protocol (W, FW, NW) and the scoring method. These correlations were calculated with eight data points corresponding to each objective compound in Supplementary Table S3.

Serie 2 (L2)			
Scoring method	r(W)	r(FW)	r(NW)
P5	0.78	0.75	0.65
P25	0.72	0.83	0.58
MBE	0.78	0.84	0.80
POP5	0.76	0.61	0.63
POP25	0.73	0.63	0.50
POPMBE	0.73	0.61	0.48

**Table S7.** Correlation between the experimental data in the literature and predicted data depending on the protocol (W, FW, NW) and the scoring method. These correlations were calculated with seven data points corresponding to the first seven objective compounds in Supplementary Table S4.

Serie 3 (L3)			
Scoring method	r(W)	r(FW)	r(NW)
P5	0.58	0.39	0.24
P25	0.46	0.29	0.31
MBE	0.48	0.30	0.27
POP5	0.58	0.32	0.31
POP25	0.44	0.20	0.31
POPMBE	0.50	0.16	0.22

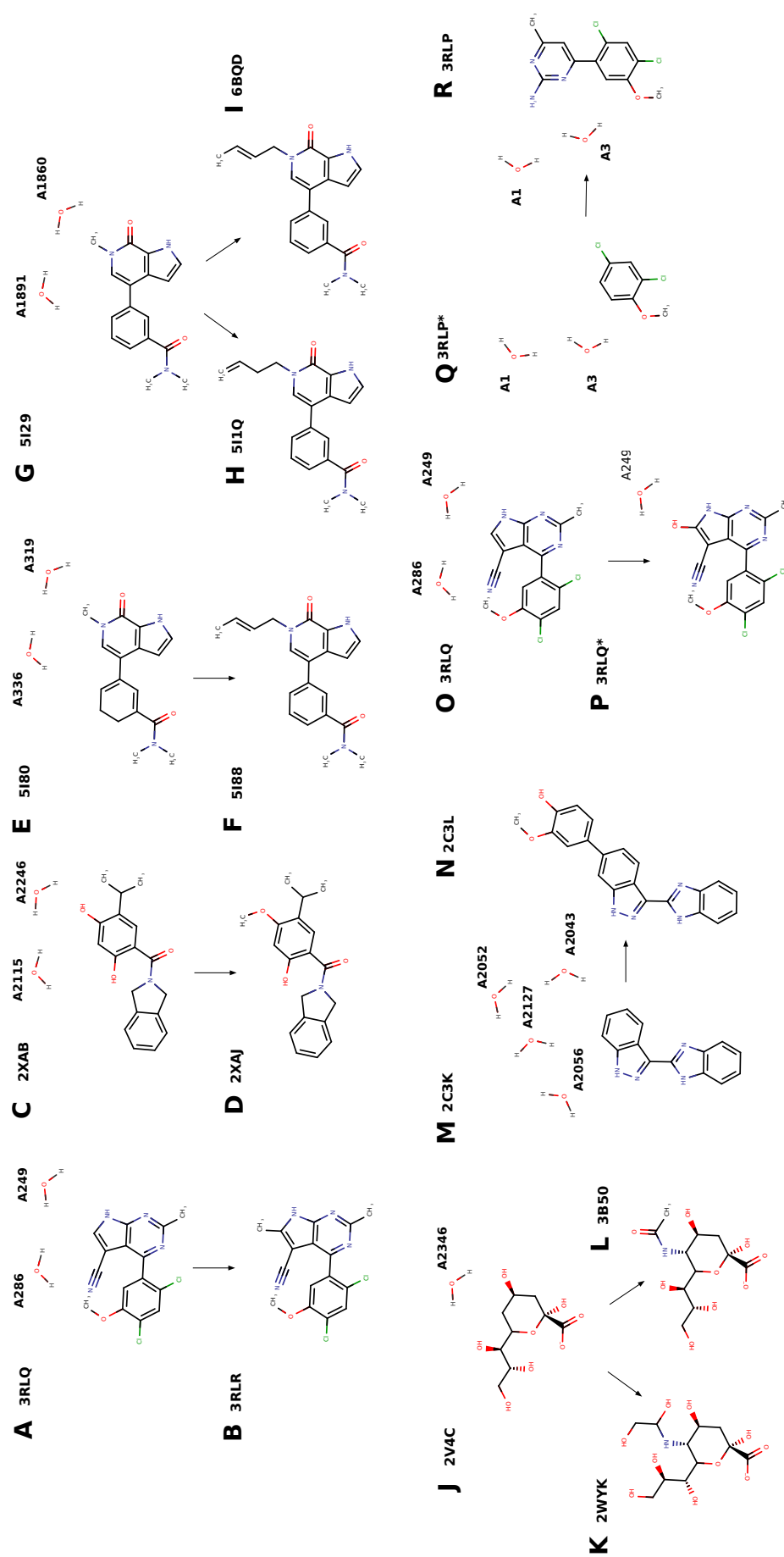


**Figure S1.** Set of systems considered in the structural study benchmark. PDB codes are indicated along with the labelling of each ligand structure. It has binders to the HSP90 (panels A-D and O-R), BRD4 (E and F), TAF1 (G-I), SiaP WT (J-L) and CHK1 (M and N) [43–47] Water molecules have been labelled according to the indicated PDB. \*Structure that doesn't have a crystal but has been modified from the indicated PDB.

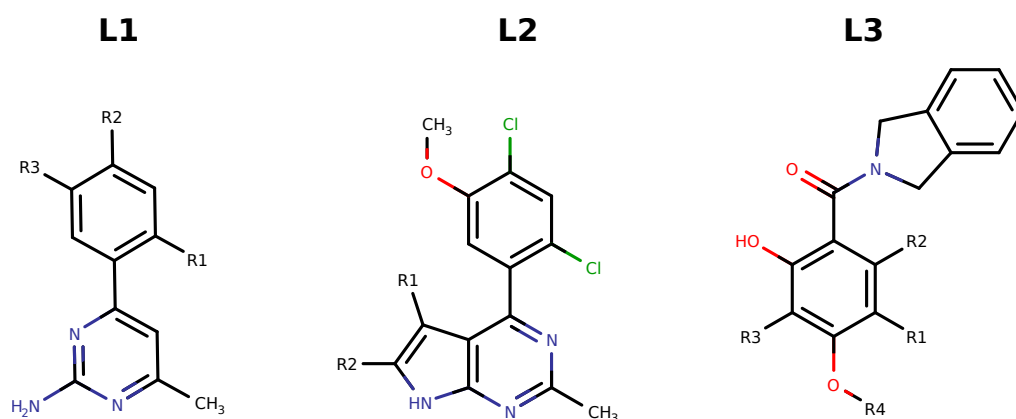


**Figure S2.** Set of initial scaffolds considered in the energetic study benchmark. These HSP90 inhibitors have not been crystallized in complex with the protein. R1, R2, R3 and R4 indicate regions where the fragments from the Supplementary Tables S2, S3 and S4 are going to be grown. Compounds and energetic data have been retrieved from the literature [43,44].